Journal of Nuclear Materials 386–388 (2009) 974–978

Contents lists available at ScienceDirect

Journal of Nuclear Materials

journal homepage: www.elsevier.com/locate/jnucmat

Statistical evaluation of anisotropic fracture behavior of ODS ferritic steels by using small punch tests

Naoyuki Okuda [a], Ryuta Kasada [b,*], Akihiko Kimura [b]

[a] Graduate School of Energy Science, Kyoto University, Uji, Kyoto, Japan
[b] Institute of Advanced Energy, Kyoto University, Gokasho, Uji, Kyoto 611-0011, Japan

ARTICLE INFO

PACS:
62.20.Mk
68.55.Jk

ABSTRACT

Small punch (SP) tests were performed to evaluate the anisotropy in the ductile–brittle transition behavior for the oxide dispersion strengthened (ODS) ferritic steel for the advanced nuclear systems. The upper-shelf energy and scattering of SP fracture energy for the specimens where the surfaces are perpendicular to the extruded direction was larger and smaller than that for the other direction, respectively. The anisotropic fracture behavior appears to be mainly caused by the favorable cracking path along the elongated grain. Data scattering of SP fracture energy could be explained by combination of microstructural observations and the statistical evaluation method based on the Weibull distribution of SP fracture energy, indicating that brittle inclusions along elongated grain was responsible to the unexpected initial failure type fracture mode.

1. Introduction

Oxide dispersion strengthened (ODS) ferritic steels are being developed for high-temperature components in fusion reactors as well as next generation fission reactors [1,2]. While the ODS ferritic steels have shown excellent creep strength and irradiation resistance, the mechanical properties, such as tensile properties, fracture toughness and creep rupture, of the ODS ferritic steels have occasionally shown anisotropic behavior due to the texture formation during hot-extrusion processing [3–6]. The authors showed that the fracture strain of tensile tests on ODS ferritic steels depended on the directionality of the specimens cut from extruded bars [6]. Alinger et al. showed that MA957 in the form of extruder bar had a strong anisotropy of fracture toughness evaluated by using three-point bend specimens [4].

Small punch (SP) test have been developed and used for the evaluation of mechanical properties, such as the ductile–brittle transition behaviors [7,8], fracture toughness [9], and high-temperature strength [10], for fusion reactor structural materials. In addition to these works, SP test is convenient for evaluating anisotropic ductile–brittle transition behavior of thin component, typified by pipes made by the hot-extruded ODS ferritic steels. Furthermore, SP tests using typically 3 mm diameter disks for transmission electron spectrometry (TEM) can drastically reduce the specimen volume for irradiation experiments in the IFMIF project. The key issue for utilization of the SP tests for the above-mentioned studies is to establish a statistical model to suitably fit data obtained from small specimens.

The present work shows the SP test results of anisotropic fracture behavior of the hot-extruded ODS ferritic steel. The data scatter problem of SP tests to evaluate the ductile–brittle transition behavior of ODS ferritic steels was also discussed by using statistical evaluation methods based on the Weibull distribution of SP fracture energy.

2. Experimental procedures

The material used in the present study is the K2 ODS ferritic steel developed by Kyoto University collaboratively with KOBELCO Research Institute, Inc. The chemical composition of K2 ODS ferritic steel is Fe(bal.)–13.64Cr–4.12Al–1.65W–0.28Ti–0.381Y_2O_3 in wt.% [3]. Mechanical alloying processing by using an attrition mill and following hot-extrusion processing was applied to fabricate the K2 ODS ferritic steel. The hot-extrusion was carried out at 1150 °C. The final heat treatment is 1050 °C for 1 h followed by air-cooling.

SP tests were carried out on 3 mm diameter × 0.23 mm thickness disk specimens punched put from the sheets in two orientations with respect to the extrusion direction: (a) the sheet surface is parallel to longitudinal direction of the extruded bar (named as L-direction); (b) the sheet surface is normal to longitudinal direction of the extruded bar (T-direction). The crosshead speed during deformation was 0.2 mm/min in the temperature range from −192 °C to 30 °C. The punch deformation was achieved by pushing 1 mm diameter hard steel ball on the surface of the specimen clamped between upper and lower dies. Detail of the

* Corresponding author. Tel.: +81 774 38 3483; fax: +81 774 38 3479.
E-mail address: r-kasada@iae.kyoto-u.ac.jp (R. Kasada).

0022-3115/$ - see front matter © 2008 Elsevier B.V. All rights reserved.
doi:10.1016/j.jnucmat.2008.12.265

punch fixture used was shown in Ref. [8]. The load-deflection curves were recorded and the SP fracture energy was calculated as the area bounded by the load-deflection curve. As shown by Misawa et al. [7], Weibull distribution was suitable for dealing with variability in SP fracture energy. The distribution function $F(E)$, mean value μ and dispersion σ are given in the following two-parameter Weibull statistical model:

$$F(E) = 1 - \exp(-E/E_0)^m, \quad (1)$$

$$\mu = E_0[\Gamma(1 + 1/m)], \quad (2)$$

$$\sigma = E_0[\Gamma(1 + 2/m) - \Gamma^2(1 + 1/m)]^{1/2}, \quad (3)$$

$$\Gamma(u) = \int_0^\infty x^{u-1} e^{-x} dx, \quad (4)$$

where E is the SP fracture energy normalized by the specimen thickness, E_0 is the scale parameter and m is the shape parameter in the Weibull distribution. The obtained data E at each testing temperature were ranked in ascending order and assigned a cumulative probability value concerning the following ranking equation:

$$F(E) = (i - 0.5)/n, \quad (5)$$

where i is the rank order number, from 1 to n, and n is the total number of E data. Following SP tests, the fracture surface of selected specimens was observed by using scanning electron microscopy (SEM).

3. Results and discussion

3.1. Anisotropic fracture behavior of ODS ferritic steel evaluated by SP test

Fig. 1 shows examples of load-deflection curves for SP tests at room temperature of the ODS ferritic steel for (a) L-direction and (b) T-direction. The curve is quite different between the directions, resulting larger maximum strength and deflection for the T-direction. Fig. 2 shows all data sets of SP fracture energy normalized by the specimen thickness for (a) L-direction and (b) T-direction with a line connected of mean value μ at each testing temperature. As can be clearly seen, data scattering and transition temperature range is larger for the L-direction than for the T-direction. Even in the upper-shelf region of the T-direction, however, there was a small number of lower SP fracture energy data close to zero. Since these lower SP fracture energy should reflect changes in fracture mode, SEM observations were performed on the fracture surfaces. Fig. 3 is the SEM images for the specimens showing the low SP fracture energy data of (a) L-direction tested at −191 °C and (b) T-direction tested at −153 °C. The macroscopic cracking direction in the both directions appears to reflect the extrusion direction such as a cross-shape for the T-direction and a line-shape for the L-direction. The fracture surface of both directions are showing cleavage mode. At the initiation site of brittle fracture, furthermore, large inclusions were observed on the fracture surface as given in Fig. 3(a-3) and (b-3). With considering that similar inclusions such as impurity oxide, carbide, and unmixed source powders were observed and analyzed in another ODS ferritic steels [4,11], these coarsened inclusions must be trigger of the brittle fracture showing the low SP fracture energy. Namely, reduction of these unexpected features can probably improve the fracture probability of ODS ferritic steels at low temperatures.

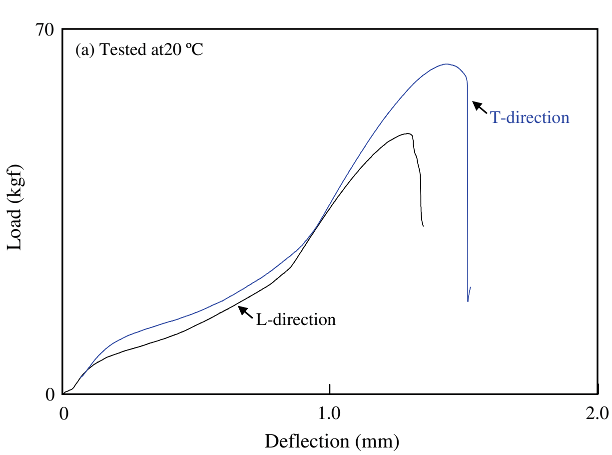

Fig. 1. Examples of load-deflection curves for L-direction and T-direction of ODS ferritic steel tested at 20 C.

As the test temperature increased from the transition region to the upper-shelf region, the ratio of brittle cleavage decreases with decreasing of contribution of the coarsened inclusions, and ductile failure occurs at the upper-shelf region. The load-deflection curves shown in Fig. 1 indicate that the difference of upper-shelf energy between L-direction and T-direction should be due to the anisotropy in the plastic ductility and strength during the membrane stretching. Fig. 4 shows the appearance and fracture surface of the L- and T-directions ruptured at a level of the upper-shelf energy. While both the specimens showed the ductile stretching behavior at the circumstance area touching with the indentation ball, different manner of the cracking was observed in the Fig. 4(a-1) and (b-1). While the L-direction showed a line-shape cracking as well as the brittle fracture in Fig. 3(a-1), the T-direction have many tiny cracking to penetrative cracking for the thickness-direction of the specimen. These behaviors indicate that the crack propagation along the extrusion-direction is favorable for the present hot-extruded ODS ferritic steels. In our previous study, tensile test results of the similar ODS ferritic steels clearly showed that the fracture strain of the specimen tensioned as to be perpendicular to the direction of hot-extrusion was smaller than that of the specimens tensioned as to be parallel to the direction of hot-extrusion [6]. We have confirmed that the extrusion direction was parallel to <1 1 0> in the similar ODS ferritic steel made by same procedure; that is, fiber texture was formed [11]. Baczynski et al. indicated that the distribution of {1 1 0} and {1 1 2} slip planes available to participate in the ductile fracture process was important to understand the anisotropy of ductile fracture for the rolled high-strength low-alloy pipeline steels [12]. In addition to this anisotropic deformation behavior of the textured ferritic steel, coarsened brittle phases along the elongated grain, such as carbides and oxide, probably play an important role in the anisotropic cracking behavior. Further investigation is underway to understand and decrease the anisotropy.

3.2. Statistical analysis of SP test results

Statistical analysis based on the Weibul model was applied to determine the ductile–brittle transition temperature (DBTT) from the present SP test results showing relatively large scattering. Here, the DBTT was determined as the temperature corresponding to the half value of ductile upper-shelf region of the mean values. As the results, the DBTT is slightly lower for the L-direction (−153 °C) than for the T-direction (−145 °C) and the upper-shelf energy is obviously higher for the T-direction than for the L-direction. The dispersion σ has a peak around the DBTT as expected. Our previous study showed an empirical relationship between the DBTT values of Charpy impact tests (CVN–DBTT) from those of SP tests (SP–DBTT) as SP–DBTT = 0.4 × CVN–DBTT [13]. The difference of CVN–DBTT between the L-direction and T-direction evaluated from the relationship was 20 °C, which was not so far from the difference of temperature shift for fracture toughness of MA957 between C and R orientation (the crack propagation mode is similar

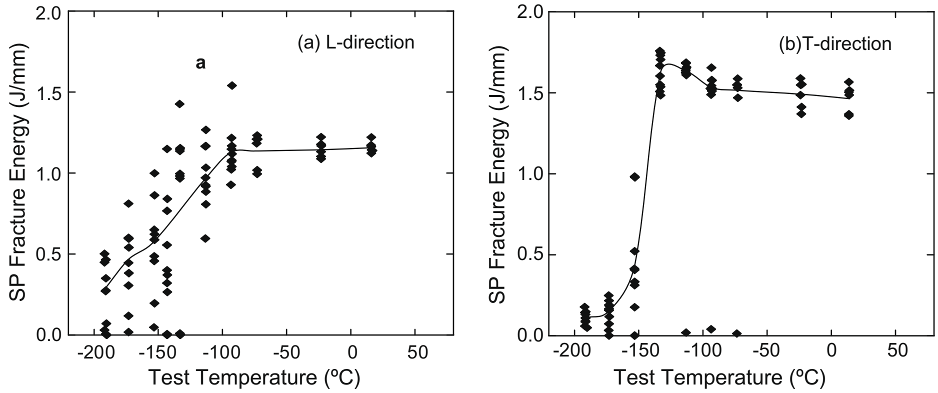

Fig. 2. Test-temperature dependence of SP fracture energy normalized by specimen thickness of (a) L-direction and (b) T-direction of ODS ferritic steel with each mean value line.

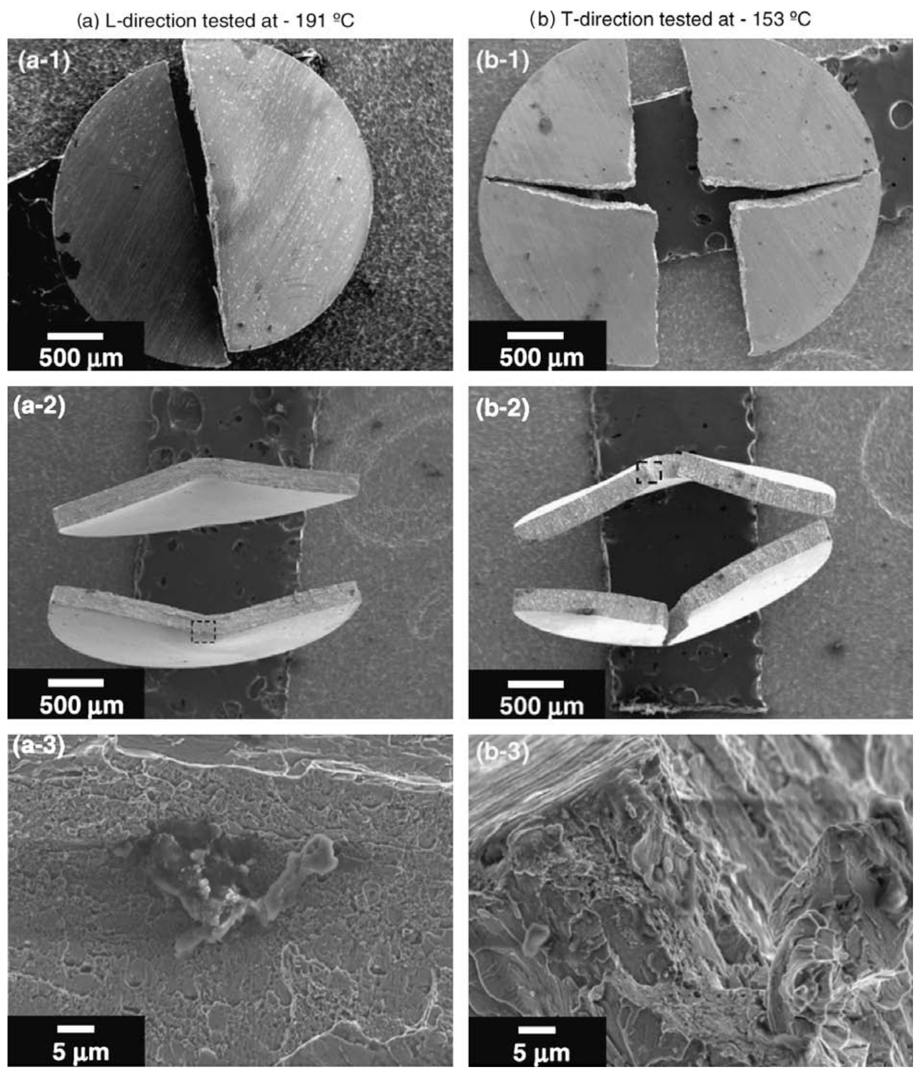

Fig. 3. SEM fractograph of ODS ferritic steel after SP tests at (a) −191 C for L-direction and (b) −156 C for T-direction.

to the current L-direction) and C–L orientation (the crack propagation mode is similar to the current T-direction) [4]. However these considerations are effective only when a large number of SP tests at multiple temperatures were performed like the present paper.

To estimate the scatter of SP fracture data statistically, the examples of Weibull probability plots, i.e., ln $[1/(1-F(E))]$ versus ln E, were given in Fig. 5(a) L-direction and (b) T-direction. A single distribution was observed for the L-direction tested at −23 °C and for the T-direction tested at −191 °C and −23 °C. On the other hand, the distribution appears to be composite when the SP tests were carried out at temperatures in the transition range. In these conditions, the multiple m values were determined from the gradi-

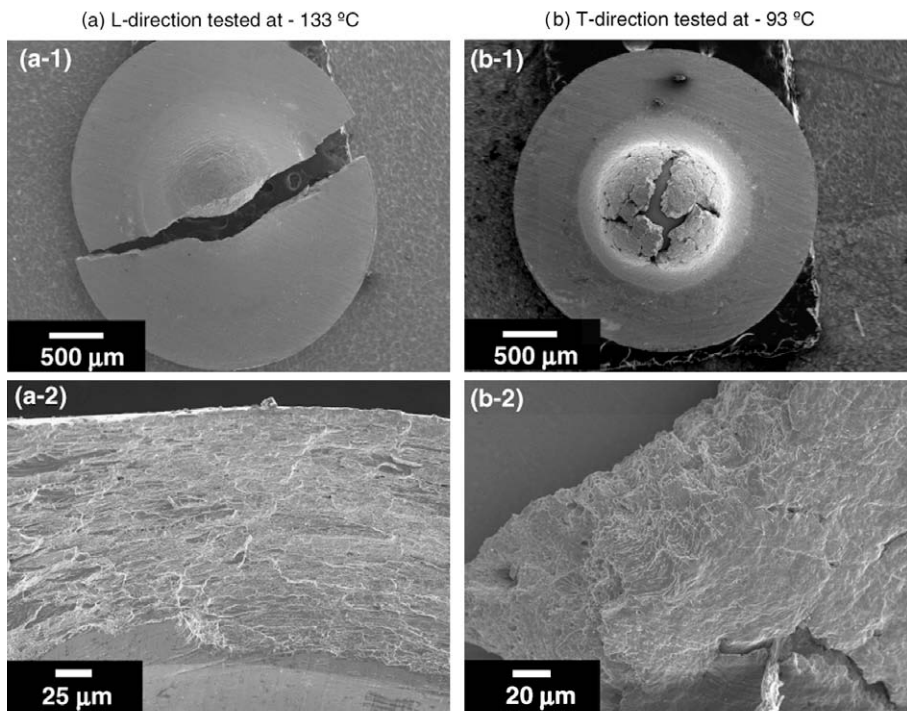

Fig. 4. SEM fractograph of ODS ferritic steel after SP tests at (a) −133 C for L-direction and (b) −93 C for T-direction.

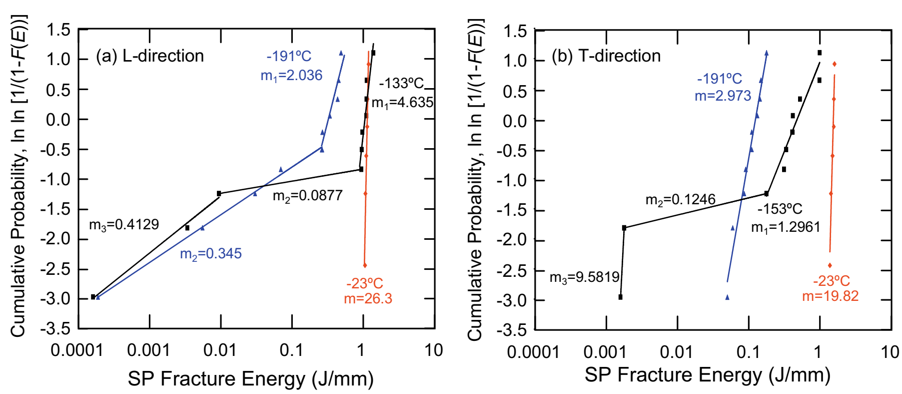

Fig. 5. Weibull plots of SP fracture energy normalized by specimen thickness of (a) L-direction and (b) T-direction.

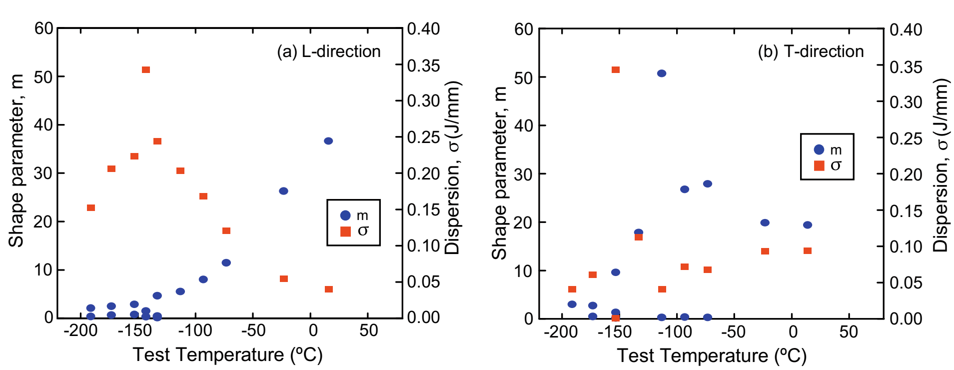

Fig. 6. Temperature dependence of Weibull shape parameter and dispersion of (a) L-direction and (b) T-direction.

ents of the multiple lines by using the least mean square method. The temperature dependences of the shape parameter and the dispersion obtained from K2 ODS ferritic steel were shown in Fig. 6. The initial failure type values, i.e., $m \leqslant 1$, were observed with corresponding to the small number of low SP fracture energy data close to zero within the brittle to transition temperature range and some of ductile range for T-direction. While the accuracy of the low m value is very low, the origin of the initial failure type fracture must be due to coarsened brittle phase as shown in Fig. 3. The m value of L-direction gradually increased up to $m \approx 10$ with increasing test temperature from lower-shelf region to transition region up to -73 °C. On the upper-shelf-region, furthermore, the m value showed significant high values which mean less scattering due to the ductile failure. On the other hand, the m value of T-direction reached to $m \approx 10$ at -153 °C. Except for some initial failure type fracture data, significant high values due to the ductile failure was also observed in the T-direction tested at temperatures above -133 °C. The temperature dependence of the m values is quite different with that of the mean value curve. It can be concluded that a simple definition of DBTT for L-direction with small number of SP specimens is difficult due to the wide transition temperature range with large scattering when compared with the T-direction. However these scattering of brittle fracture behavior for the L-direction must be taken into accounts in the view point of practical use of extruded ODS ferritic steels as fuel cladding and thin wall components.

4. Conclusions

The SP tests were examined for evaluating the anisotropic ductile–brittle transition behavior of K2 ODS ferritic steel with consideration of the Weibull statistical analysis. The results obtained are summarized as follows:

(1) The SP tests demonstrated that the DBTT for the L-direction was slightly lower than for the T-direction and the upper-shelf energy for the L-direction was lower than for the T-direction.

(2) The anisotropic fracture behavior is due to the favorable cracking path along the direction of the elongated grain of the extruded ODS ferritic steels.

(3) Data scattering of SP fracture energy could be explained by the statistical evaluation method based on the Weibull distribution of SP fracture energy. Microstructural observations on the fracture surfaces well supported the model to explain the initial failure type fracture mode probably due to brittle inclusions.

References

[1] A. Kimura, R. Kasada, A. Kohyama, H. Tanigawa, T. Hirose, K. Shiba, S. Jitsukawa, S. Ohtsuka, S. Ukai, M.A. Sokolov, R.L. Klueh, T. Yamamoto, G.R. Odette, J. Nucl. Mater. 367–370 (2007) 60.
[2] A. Kimura, H.S. Cho, N. Toda, R. Kasada, K. Yutani, H. Kishimoto, N. Iwata, S. Ukai, M. Fujiwara, J. Nucl. Sci. Technol. 44 (3) (2007) 323.
[3] H.S. Cho, R. Kasada, A. Kimura, J. Nucl. Mater. 367–370 (2007) 239.
[4] M.J. Alinger, G.R. Odette, G.E. Lucas, J. Nucl. Mater. 307–311 (2002) 484.
[5] H. Okada, S. Ukai, M. Inoue, J. Nucl. Sci. Technol. 33 (12) (1996) 936.
[6] R. Kasada, N. Toda, H.S. Cho, A. Kimura, Tensile deformation behavior of oxide-dispersion strengthened ferritic steels, in: Proceedings of the American Nuclear Society – International Congress on Advances in Nuclear Power Plants 2005, ICAPP'05 3, pp. 1703–1711.
[7] T. Misawa, T. Adachi, M. Saito, Y. Hamaguchi, J. Nucl. Mater. 150 (1987) 194.
[8] R. Kasada, T. Morimura, A. Hasegawa, A. Kimura, J. Nucl. Mater. 299 (2001) 283.
[9] T. Misawa, S. Nagata, N. Aoki, J. Ishizawa, Y. Hamaguchi, J. Nucl. Mater. 169 (1989) 225.
[10] T. Nakata, S.-I. Komazaki, M. Nakajima, Y. Kohno, H. Tanigawa, K. Shiba, A. Kohyama, J. Jpn. Inst. Met. 70 (2006) 642.
[11] R. Kasada, S.G. Lee, A. Kimura, submitted for publication.
[12] G.J. Baczynski, J.J. Jonas, L.E. Collins, Metall. Mater. Trans. A 30 (1999) 3045.
[13] A. Kimura, T. Morimura, R. Kasada, H. Matsui, A. Hasegawa, K. Abe, ASTM STP 1366 (2000) 626.